# A facile route for irreversible bonding of plastic-PDMS hybrid microdevices at room temperature†

## Linzhi Tang and Nae Yoon Lee*

Plastic materials do not generally form irreversible bonds with poly(dimethylsiloxane) (PDMS) regardless of oxygen plasma treatment and a subsequent thermal process. In this paper, we perform plastic-PDMS bonding at room temperature, mediated by the formation of a chemically robust amine–epoxy bond at the interfaces. Various plastic materials, such as poly(methylmethacrylate) (PMMA), polycarbonate (PC), polyimide (PI), and poly(ethylene terephthalate) (PET) were adopted as choices for plastic materials. Irrespective of the plastic materials used, the surfaces were successfully modified with amine and epoxy functionalities, confirmed by the surface characterizations such as water contact angle measurements and X-ray photoelectron spectroscopy (XPS), and chemically robust and irreversible bonding was successfully achieved within 1 h at room temperature. The bonding strengths of PDMS with PMMA and PC sheets were measured to be 180 and 178 kPa, respectively, and their assemblies containing microchannel structures endured up to 74 and 84 psi (510 and 579 kPa) of introduced compressed air, respectively, without destroying the microdevices, representing a robust and highly stable interfacial bonding. In addition to microchannel-molded PDMS bonded with flat plastic substrates, microchannel-embossed plastics were also bonded with a flat PDMS sheet, and both types of bonded assemblies displayed sufficiently robust bonding, tolerating an intense influx of liquid whose per-minute injection volume was nearly 1000 to 2000 times higher than the total internal volume of the microchannel used. In addition to observing the bonding performance, we also investigated the potential of surface amine and epoxy functionalities as durable chemical adhesives by observing their storage-time-dependent bonding performances.

## Introduction

The bonding of two substrates to form a closed microchannel system is essential in microfluidic related research. However, the bonding of glass-based or Si/SiO$_2$-based microdevices requires complicated procedures such as anodic or fusion bonding, which require high-temperature and high-pressure conditions as well as the application of voltage. For this reason, poly(dimethylsiloxane) (PDMS) has been widely adopted based on its simple and robust bonding at relatively low temperatures.

The bonding of silicon-based substrates such as a PDMS–PDMS homogeneous assembly, along with PDMS–glass, PDMS–quartz, and PDMS–silicon heterogeneous assemblies, are easily realized by the hydroxylation of the surfaces *via* plasma treatment, generally followed by mild heating. Along with easy and robust bonding ability, PDMS is highly advantageous for its simple fabrication, high optical transparency, and low cost.

However, the hydrophobic surface property of PDMS sometimes makes it difficult for biomolecule patterning and liquid introduction.

As an alternative to PDMS, plastic materials are also widely adopted for their low production costs, easy fabrication processes, and potential to integrate with microelectronic technologies. Microchannels are easily replicated *via* hot embossing[1–3] or injection molding[4,5] with a high feature resolution, and their surfaces are generally less hydrophobic compared to that of PDMS, which can be a great advantage for the introduction of liquid into a microchannel, and for biomolecule patterning purposes. Despite the many advantages of plastic materials, however, the bonding of two homogeneous or heterogeneous plastic materials entails complicated bonding procedures.

Many researchers have tried to fabricate plastic-based microdevices by bonding homogeneous or heterogeneous pairs of plastic materials by means of thermal bonding,[1,6–8] solvent bonding,[9] lamination,[10,11] or adhesive tape.[12] Thermal bonding was realized by heating the plastic materials above their glass transition temperature ($T_g$). This method is highly advantageous when bonding a pair of homogeneous assemblies.

However, when bonding heterogeneous assemblies, channel structures can deform or collapse in the process of heating because of their different $T_g$, therefore requiring delicate temperature and pressure control to achieve high-resolution channel profiles. For this reason, many researchers have been

*Gachon BioNano Research Institute & Division of BioNano Technology and College of BioNano Technology, Kyungwon University, San 65 Bokjeong-dong, Sujeong-gu, Seongnam, Gyeonggi-do, 461-701, Korea. E-mail: nylee@kyungwon.ac.kr; Fax: +82-31-750-8774; Tel: +82-31-750-8556*
† Electronic supplementary information (ESI) available: Supplementary video showing high-speed influx of a blue ink solution into the microdevice assembled by bonding microchannel-molded PDMS with a flat PC. See DOI: 10.1039/b924753j

working towards establishing a bonding method that is applicable at relatively lower temperature conditions. Some researchers have used PDMS as an intermediate layer to bond an embossed plastic substrate with a flat plastic substrate.[13–16] Nevertheless, a PDMS intermediate-layer-based bonding method still requires a slightly increased temperature (~90 °C) and pressure for the bonding,[14,16] and a high-resolution channel profile is not guaranteed as the uncured PDMS can flow into the microchannel during the heating process. Therefore, the issues of applying external heat and pressure, as well as the incorporation of an alienated coating layer between the two homogeneous or heterogeneous plastic substrates, must be resolved in order to obtain complete and robust bonding with high channel fidelity.

The bonding of plastic substrates to an elastomeric PDMS substrate poses versatile advantages. In addition to achieving high-resolution channel profiles due to high conformity, the elastomeric nature of PDMS can ensure complete filling of the liquid inside the microchannel without generating dead volume space, and enables the fabrication of microfluidic components such as microvalves and micropumps which can be actuated solely by delicate pressure control. In addition, a plastic–PDMS assembly is better suited in comparison to a PDMS–PDMS assembly for performing cell-based research inside a microchannel owing to its less hydrophobic surface property and the diverse availability of surface functionalities originating from the material's versatility. However, the permanent bonding of plastic materials with PDMS is difficult to realize even after the hydroxylation of the surface *via* plasma treatment followed by thermal curing. Few works[17] have been reported on the bonding of PDMS with plastic substrates that are non-silicon based, and some non-silicon based plastic materials, such as poly(methylmethacrylate) (PMMA), polyimide (PI), polycarbonate (PC), and Saran Wrap, have been shown to be unsuccessful in realizing irreversible bonding *via* an oxygen plasma treatment method.[18]

In this study, we apply a chemical gluing strategy[19] for the permanent bonding of non-silicon based plastic substrates with silicon-based PDMS at room temperature. In brief, chemical gluing is achieved by anchoring amine-terminated silane reagents on one substrate, and epoxy-terminated silane reagents on the other substrate, *via* a silane coupling reaction, followed by amine–epoxy bond formation at the interfaces at room temperature. Using this method, we have successfully demonstrated the bonding of two PDMS substrates.[19] In this study, various plastic substrates, such as PMMA, PI, PC, and poly(ethylene terephthalate) (PET) are investigated, all of which are well-known to have difficulty in bonding irreversibly with PDMS. In addition, various aminosilanes and epoxysilanes are investigated as candidates for chemical adhesives. We demonstrate the suitability of the chemical gluing strategy for obtaining robust and irreversible chemical bonding between PDMS and plastic substrates by performing a peel test, delamination test, and high-throughput leakage test, and characterize the surface functionalities through contact angle measurement and X-ray photoelectron spectroscopy (XPS) analysis. Furthermore, we examine the feasibility of the anchored surface functionalities for use as long-lasting chemical adhesives.

## Experimental

### Chemicals and materials

SU-8 2150 and SU-8 developer were purchased from MicroChem (Newton, MA, USA). Poly(dimethylsiloxane) (PDMS) prepolymer (Sylgard 184) and a curing agent were purchased from Dow Corning (Midland, MI, USA). 3-Aminopropyltriethoxysilane (APTES, 99%), 3-aminopropyltrimethoxysilane (APTMS, 97%), and 3-glycidoxypropyltrimethoxysilane (GPTMS, 98%) were purchased from Aldrich. 3-Glycidoxypropyltriethoxysilane (GPTES), 3-glycidoxypropylmethyldiethoxysilane (GPMDES), and n-octyltriethoxysilane were purchased from Gelest. N-2(Aminoethyl)3-aminopropyltrimethoxysilane (KBM-603) was purchased from ShinEtsu. PI film (Kapton E, 38 μm) was purchased from DuPont, and PET film (180 μm) was purchased from SKC (Korea). PMMA and PC sheets both with thicknesses of 3 mm and PC film with thickness of 0.5 mm were used. NOA (Norland Optical Adhesive) 63 was purchased from Norland Company.

### Microchannel fabrication

Serpentine microchannels were fabricated on both PDMS and plastic substrates. First, to fabricate a PDMS microchannel, conventional photolithography and replica molding techniques were used. SU-8 2150 was spin-coated on a plasma-treated Si (100) wafer at 3000 rpm for 30 s, followed by soft baking at 65 °C for 5 min, and at 95 °C for 30 min. After UV exposure for 15 s (365 nm, 15 mW cm$^{-2}$) using a mask aligner (CA-6M, Shinu M.S.T, Korea), hard baking was performed at 65 °C for 5 min, and at 95 °C for 15 min. After development in an SU-8 developer, the SU-8 master mold was thoroughly washed in isopropyl alcohol and dried. A 10 : 1 (w/w) mixture of the PDMS prepolymer and a curing agent was degassed and then poured onto the SU-8 master mold. After thermal curing at 80 °C for 30 min, the PDMS replica mold was peeled off the master mold.

Next, to fabricate a microchannel on plastic substrates, a hot embossing process[20] was used. Fig. 1 shows a photo of the custom-made pneumatic press machine and a schematic for the hot embossing process. To obtain a template for hot embossing, a UV-curable NOA 63 prepolymer[21] was employed to fabricate a negative replica structure from the PDMS replica mold. To fabricate a flexible NOA 63 template, NOA 63 precursor was poured into the microchannel-molded PDMS and degassed to
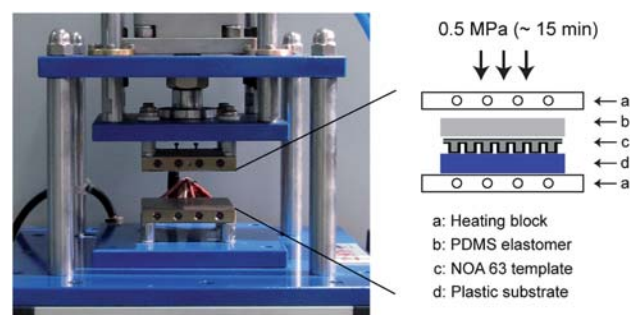


**Fig. 1** Photo of the custom-made pneumatic press machine and a schematic for the hot embossing process performed at 0.5 MPa for 15 min.

completely remove air bubbles, followed by a conformal contact of the NOA 63-filled PDMS with a NOA 63-coated PET substrate. Upon UV photopolymerization (135 mW cm$^{-2}$) overnight, the surface of the NOA 63 template was passivated using n-octyltriethoxysilane for the easy release of the template from the embossed plastic substrate. A flat plastic sheet was placed at the bottom, and the NOA 63 template was placed atop the plastic sheet. A thin flat PDMS with a homogeneous thickness of 2.5 mm was placed on top of the assembly to aid in the conformal contact of the plastic substrate with the NOA 63 template, as well as for an efficient pressure distribution during the embossing process. Considering that the $T_g$ values of PMMA and PC are 105 °C and 148 °C, respectively, both the top and bottom blocks were identically heated at 95 °C and 135 °C for PMMA and PC, respectively. The embossing pressure and time were controlled to be 0.5 MPa and 15 min for both substrates.

### Bonding strategy

Fig. 2 shows the basic concept of the chemical gluing at room temperature.[19] First, the surfaces of the PDMS replica and a flat plastic substrate were treated with oxygen ($O_2$) plasma (50–60 W) for 1 min (Fig. 2(a)). After generating hydroxyl groups on the surfaces of both substrates, 1% (v/v) aqueous solutions of aminosilane and epoxysilane were poured and reacted for 20 min to generate surface amine and epoxy functionalities (Fig. 2(b)). After a thorough washing and drying, the solution-treated surfaces were bonded for 1 h at room temperature (Fig. 2(c)) to form a strong amine–epoxy bond.

### Surface characterizations

**Contact angle measurement.** The water contact angles were measured on the surfaces of pristine substrate, $O_2$ plasma-treated substrate, amine-functionalized substrate, and epoxy-functionalized substrate by the sessile drop technique using a Phoenix 300



**Fig. 2** (a) Surface hydroxylation of PDMS and plastic substrates by $O_2$ plasma treatment for 1 min. (b) Aminosilane and epoxysilane anchoring on the $O_2$ plasma-treated PDMS and plastic substrates, respectively. (c) Conformal contact of the two substrates at room temperature for 1 h.

contact angle measuring system (Surface Electro Optics, Korea), and analyzed with ImagePro 300 software. Five measurements were made and averaged.

**XPS analysis.** X-ray photoelectron spectroscopy (XPS) analyses were conducted using a PHY 5700 (PHI, Chanhassen, MN, USA) equipped with an aluminium X-ray radiation source (1486.6 eV) and pass energy of 23.5 eV. The pressure in the chamber was below $1.3 \times 10^{-9}$ Torr before the data were taken, and the voltage and current of the anode were 15 kV and 26.7 mA, respectively. The take-off angle was set at 45°. The binding energy of Au $4f_{7/2}$ (84.0 eV) was used as the reference. The resolution for the measurement of the binding energy was about ±0.6 eV. XPS analyses were interpreted using an ESCA1 (PHI, Chanhassen, MN, USA).

### Bonding strength analysis

**Peel test.** A peel test was conducted using a texture analyzer (QTS 25, Brookfield, Middleboro, MA, USA) on the PDMS–PMMA and PDMS–PC (sheet) assemblies. Thick twine was inserted into the PDMS prepolymer during the thermal curing process to hold the PDMS at one end. Two holes were punctured in each plastic sheet using a sand blaster (Swam Blaster, Crystal Mark, Glendale, CA, USA) filled with aluminium oxide particles (50 μm), and two strands of thick twine were passed through the holes to hold the plastic sheet at the other end. After bonding, the assembly was pulled apart at a speed of 100 mm min$^{-1}$. In addition to performing the peel test, a delamination test was also conducted manually on the PDMS–PET, PDMS–U-PET, PDMS–PI, and PDMS–PC (film) assemblies due to their highly flexible and thin nature. At least five sets of identical experiments were conducted for each assembly for reproducibility.

**Leakage test.** Microchannel-molded PDMS was bonded to flat PMMA, PC (sheet), PC (film), PET, and U-PET substrates, and the microchannel-embossed PMMA and PC sheets were bonded to the flat PDMS, employing the chemical gluing process. Leakage tests were performed by introducing ink solutions through silicone tubes (o.d. 2.0 mm, i.d. 1.0 mm) inserted into the PDMS, and the interfaces were glued using a 10 : 3 (w/w) mixture of the PDMS prepolymer and a curing agent, and then left at room temperature overnight to eliminate the heating effect on the bonding. Both blue and red ink solutions were used for easy visualization. A syringe pump (KDS 200, KD Scientific, New Hope, PA, USA) was used to introduce ink solutions into the microchannels. The flow rates were systematically controlled at 0.15, 1.5, 15, and 30 mL min$^{-1}$, with per-minute injection volumes corresponding to 10, 100, 1000, and 2000-times the total internal volume of the serpentine microchannel used.

### Storage-time-dependent bonding

To examine the storage-time-dependent bonding performance of the chemical gluing process, the durability of the surface amine and epoxy functionalities was observed. After the surface modification with amine and epoxy functionalities, the two surfaces were kept separately inside a Petri-dish for a certain period of time, and the storage-time-dependent
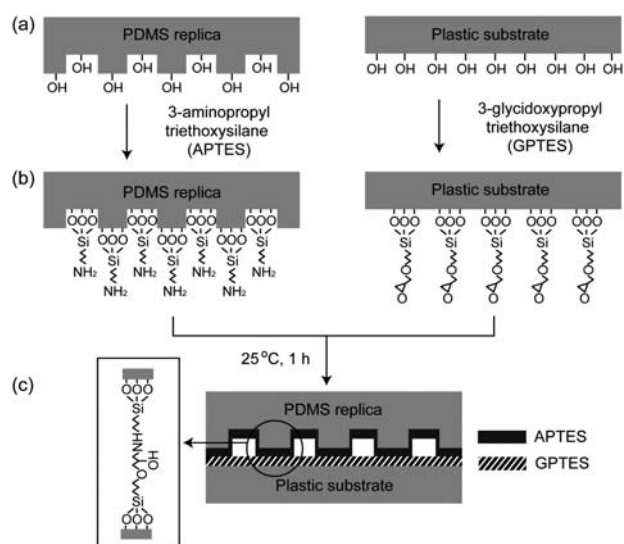
bonding performance was examined by wetting both surfaces with distilled water and drying them completely prior to the bonding.
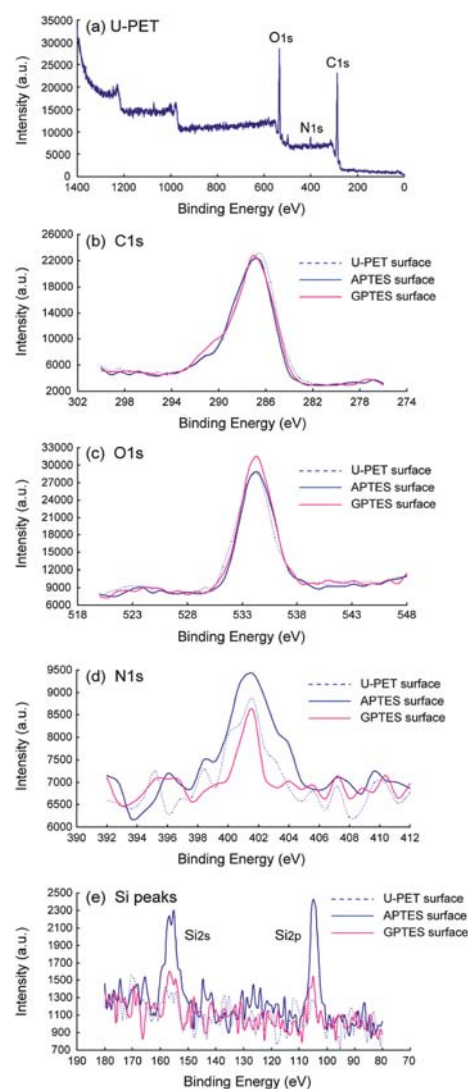
## Results and discussion

### Surface characterization

Fig. 3 shows the results of water contact angle measurements. The water contact angles on a pristine surface, $O_2$ plasma-treated surface, and APTES- and GPTES-treated surfaces of PET, U-PET, PMMA, PC (sheet), and PI are shown in Fig. 3. As shown in Fig. 3, the water contact angles of the pristine PMMA[22,23] and PC (sheet),[24,25] which can be embossed for fabricating microchannels in place of PDMS, displayed a relatively hydrophilic surface property compared to that of the pristine PDMS, which was measured to be 98.8°. After the $O_2$ plasma treatment for 1 min, the water contact angles decreased to 40–45°,[26,27] regardless of the substrate types and their original surface wettabilities, except for PI[28,29] whose water contact angle decreased to 21.5° after the $O_2$ plasma treatment. After the APTES and GPTES treatments, the water contact angles increased compared to those on the $O_2$ plasma-treated surfaces, and the increment was generally greater for APTES[30–32] than for GPTES. The decreased water contact angles after the treatments with $O_2$ plasma, APTES, and GPTES, compared with those on the pristine substrates, may be due to the introduction of polar groups and the deposition of charged functionalities. Regardless of the substrate types, the resulting contact angles seemed highly related with the anchored terminal groups.

To further confirm the successful functionalization of the plastic surfaces with amine and epoxy functionalities, XPS analyses were conducted on U-PET as shown in Fig. 4. Fig. 4(a) shows the overall element peaks detected on the surface of the pristine U-PET. PET is a polymer that is mainly composed of C, O, and H. U-PET, which is primed with a urethane functionality on the surface of PET, contains a nitrogen in its structure. Because of this, an N1s peak appears in Fig. 4(a) in addition to C1s and O1s peaks.



**Fig. 4** XPS analyses. (a) Overall element peaks detected on the surface of a pristine U-PET. (b) C1s peaks, (c) O1s peaks, (d) N1s peaks, and (e) Si peaks detected on the surfaces of pristine, APTES-anchored, and GPTES-anchored U-PET.

| | Pristine | $O_2$ plasma | APTES | GPTES |
|---|---|---|---|---|
| PET | 70.6° | 44.4° | 62.8° | 50.1° |
| U-PET | 52.5° | 40.4° | 51.6° | 46.7° |
| PMMA | 72.4° | 44.7° | 68.9° | 52.8° |
| PC | 84.3° | 40.9° | 54.0° | 45.8° |
| PI | 59.3° | 21.5° | 46.3° | 41.1° |

**Fig. 3** Water contact angles measured on pristine, $O_2$ plasma-treated, APTES- and GPTES-treated PET, U-PET, PMMA, PC, and PI substrates.
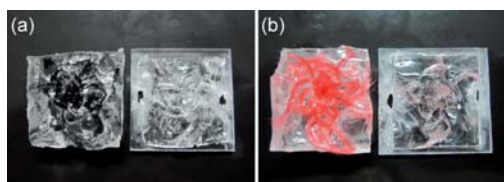
As shown in Fig. 4(b), the C1s peaks did not change notably, probably because APTES and GPTES are also composed of carbon backbones. GPTES contains an oxygen atom at its terminus, which might have attributed to the slight increase in the O1s peak for the GPTES-treated U-PET, as shown in Fig. 4(c). Since there is no oxygen atom at the terminus of APTES, the O1s peaks for the APTES-treated U-PET and a pristine U-PET were almost identical. U-PET contains a nitrogen atom on its surface which contributes to the appearance of the N1s peak (Fig. 4(a)). However, after the APTES treatment, the N1s peak intensity increased slightly, confirming the successful APTES coupling on the surface of U-PET (Fig. 4(d)). The N1s peak intensity for the GPTES-treated U-PET decreased slightly compared to that of the pristine U-PET, probably due to the masking of the surface nitrogen group in the GPTES coupling process. Fig. 4(e) shows the increased intensities of Si2p and Si2s peaks after treating the U-PET surfaces with both APTES and GPTES. This might have

resulted from the silane coupling reaction of both silanes with the hydroxylated U-PET surface. Although XPS analyses were conducted employing U-PET only in this study, we assume the XPS analysis results to be similar for all of the plastic substrates employed in this research, taking into consideration the almost identical tendencies displayed for water contact angles measured on the above-mentioned plastic substrates.
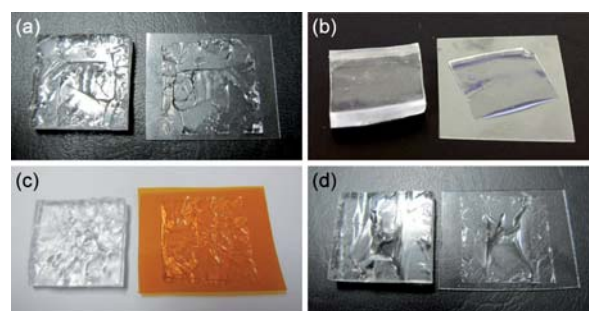
### Bonding strength analyses: Peel and delamination tests

The bonding strengths of the plastic–PDMS assemblies formed by the chemical gluing were measured by pulling two substrates apart. As shown in Fig. 5, permanent bonding was achieved regardless of the plastic substrates used, which is confirmed by the ruptured PDMS surface as well as the rugged PDMS layer attached onto the surface of the plastic substrates. The bonding strengths, defined by the strength required to pull two substrates completely apart, were measured to be approximately 180 and 178 kPa for the PDMS–PMMA and PDMS–PC (sheet) assemblies, respectively. The bonding strengths for the PDMS–PMMA and PDMS–PC (sheet) assemblies obtained were comparable to that of the PDMS–PDMS assembly obtained by the oxygen-plasma-based treatment.[33] A negative control experiment was also performed by repeating the same bonding procedures, except that the substrates were treated with distilled water that did not contain APTES or GPTES during the surface functionalization. As it turned out, bonding was not realized in the negative control experiment (data not shown). In addition to APTES and GPTES, other aminosilanes and epoxysilanes such as APTMS, KBM-603, GPTMS, and GPMDES were also used to provide versatile amine and epoxy functionalities. Irrespective of the silane sources used, bonding was successfully realized in the same manner.

For the high flexibility of PET, U-PET, PI, and PC (film), delamination tests were conducted manually in place of a peel test. As shown in Fig. 6, all of the plastic–PDMS assemblies were successfully bonded *via* chemical gluing, confirmed by their completely merged interfacial surfaces. Although the plastic substrates employed in the experiment are non-silicon based, the formation of Si–O–C and Si–O–Si bonds on the hydroxylated surfaces of the plastic and PDMS substrates, respectively, *via* silane coupling reactions, followed by a strong amine–epoxy bond formation by the terminal amine and epoxy groups of two silane reagents, might have induced strong bonding regardless of the types of plastic materials used. The fabrication of plastic–PDMS hybrid assemblies is particularly suitable when forming a PDMS-based microfluidic device using a thin and transparent covering such as PET or PC (film) substrates, targeted for cell research, as extremely thin substrate enables an efficient
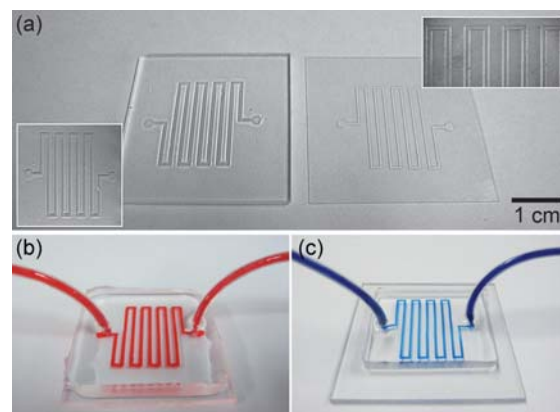


**Fig. 6** Delamination test results. Chemical gluing-based bonding of (a) PDMS–PET assembly, (b) PDMS–U-PET assembly, (c) PDMS–PI assembly, and (d) PDMS–PC (film) assembly.

observation of cells under a microscope. Also, the high flexibility of the plastic substrates resists cracking or breaking of the device, ensuring its stability. The surface functionalization using aqueous solutions of amino- and epoxysilanes does not transform the optical properties of the plastic substrates and PDMS into an opaque or frosted state, maintaining high optical transparencies for both the plastic substrates and PDMS. Also, the fast bonding of the plastic–PDMS assembly at room temperature within 1 h promises highly reliable bonding and outstanding reproducibility that is universally applicable to various hard and soft plastic substrates. Because the chemical gluing strategy ensures a simple and easy surface functionalization process employing any type of amino- or epoxysilane, not requiring an additional thermal curing procedure, the issues of channel collapse and deformation are completely resolved.

### Bonding strength analyses: leakage test

The bonding strengths of the plastic–PDMS assemblies were further examined by performing a high-throughput leakage test. A serpentine microchannel with 500 μm in width, 186 mm in total length, and 150 μm in height was successfully fabricated *via* both PDMS replica molding and hot embossing. Fig. 7(a) shows the



**Fig. 5** Peel test results. (a) PDMS–PMMA and (b) PDMS–PC (sheet) assemblies bonded by the chemical gluing at room temperature for 1 h.



**Fig. 7** Leakage test results performed at various flow rates inside a microchannel formed by the chemical gluing. (a) Microchannel-embossed PMMA (left) and a flexible NOA 63 template used for the embossing (right). (b) Red ink solution flowing into microchannel-embossed PMMA bonded with a flat PDMS. (c) Blue ink solution flowing into microchannel-molded PDMS bonded with a flat PC sheet.

microchannel-embossed PMMA (left) and flexible NOA 63 template (right) used for the embossing. As shown in Fig. 7(a), the serpentine microchannel was embossed with high-pattern fidelity without destroying the NOA template. The inset on the left shows the backside view of the embossed microchannel, and that on the right shows the enlarged edges of the microchannel patterned on the NOA 63 template. NOA 63 is an inherently hard polymer with a Young's modulus of 1655 MPa and tensile strength of 34.5 MPa.[34] To make the NOA 63 template flexible, NOA 63-based microchannel was transferred onto a flexible PET substrate on which a thin layer of the same NOA 63 was laminated. Owing to the high mechanical strength of NOA 63 and the high flexibility of a PET substrate, the NOA 63 template endured the high pressure applied during the embossing process, and could be used repeatedly without destroying the template. NOA 63 template can also be fabricated in a highly cost-effective manner.

Fig. 7(b) and (c) show the results of the high-throughput leakage tests performed inside the microchannels formed by bonding a microchannel-embossed PMMA with a flat PDMS, represented by the red ink solution (Fig. 7(b)), and a microchannel-molded PDMS with a flat PC (sheet), represented by the blue ink solution (Fig. 7(c)).

For each flow rate condition, the ink solution passed through the microchannel, without leakage. Considering that the total internal volume of the microchannel and the highest flow rate applied were approximately 15 μL and 30 mL min$^{-1}$, respectively, the bonded assembly tolerated an intense influx of ink solution whose per-minute injection volume was nearly 2000-times greater than the total internal volume of the microchannel used, without destroying the bond (see ESI†). This verifies that a robust amine–epoxy chemical bond was successfully formed in the plastic–PDMS assembly. When the flow rates were increased further, a leakage of ink occurred mostly from the disconnection of the silicone tube from the syringe, presumably due to the slippery nature of the silicone tube. When this issue was resolved through the replacement of a less slippery tube, however, the plastic–PDMS assembly could endure even higher influx of liquid into the microchannel. Although not shown here, all of the bonded assemblies successfully endured an introduction of ink, at 30 mL min$^{-1}$, regardless of the plastic materials used.

The bonding strength was also measured by flowing compressed air into the bonded microchannels. The measured average maximum leakage pressures for microchannel-molded PDMS with a series of flat PMMA, PC sheet, PET, and U-PET were 74, 84, 84, and 88 psi (510, 579, 579, and 607 kPa), respectively, which were almost equivalent to or even greater than the measured maximum leakage pressure for the PDMS–glass assembly of 75 psi.[35] The bonded assemblies of flat PDMS with microchannel-embossed PMMA and PC sheets endured an introduced air pressure of 78 and 76 psi (538 and 524 kPa), respectively. Although the bonding was still robust at those measured maximum leakage pressures, it was technically difficult to introduce a higher pressure of air due to the significant inflation of the flexible silicone tube. However, this could be easily overcome by replacing the tube with a more rigid one. Considering that the pressure generally applied inside a microchannel for fluidic experiment is typically no higher than 50 psi,[36] a chemical gluing strategy is widely applicable for realizing

a highly-robust plastic–PDMS hybrid assembly adopting a wide variety of plastic materials.

### Storage-time-dependent bonding

The time-dependent durability of the surface functionalities was investigated in order to observe how long the surface chemical functionalities can function as chemical adhesives in view of long-term stability. PDMS–U-PET assemblies were used for this experiment. Various aminosilanes and epoxysilanes were adopted to obtain a wide variety of PDMS–U-PET assemblies with diverse amine and epoxy sources. As a result, the chemical gluing-based bonding was most effective when two substrates came into contact immediately after completing the surface functionalization. The bonding performance decreased dramatically with an increased lapse of time before contact of the two substrates. However, at the expense of increased temperature (~80 °C) accompanied with the wetting process of functionalized surfaces prior to bonding, bonding was still successful, and the surface chemical functionalities were viable for up to 63 days before contact was realized. Bonding failed even when freshly oxygenated substrates were immediately assembled and heated up to 80 °C for a prolonged period of time, unless a surface functionalization step was otherwise involved. This confirms that the surface amine and epoxy functionalities acted as the key factor in realizing the bonding, and the effective duration of the surface amine and epoxy functionalities was longer than 60 days regardless of the sources of aminosilanes and epoxysilanes, but at the expense of increased temperature, however. Considering that the applied temperature (~80 °C) was still lower than the $T_g$ values of the plastic substrates used in this study and most of other plastic materials, channel fidelity was also well preserved. The long-lasting nature of the surface chemical functionalities could enable long-term storage of unassembled microdevices, and could effectively be utilized where the pre-dispensing of biomolecules or biochemical reagents, as well as the encapsulation of micro- or nanoparticles, are required in an open space prior to forming a closed microenvironment, without damaging the pre-dispensed or encapsulated materials during the bonding process.

## Conclusions

In this study, the bonding of various plastic substrates with PDMS was demonstrated by employing chemical gluing, and the robustness of the bonding was extensively studied by employing various mechanical analyses. Owing to the robust chemical bonds formed, this method is widely applicable not only for silicon-based substrates, but also for non-silicon based substrates, of which most of the plastic substrates are based. Considering that plastic materials generally have a low $T_g$, which could deform the plastic materials at relatively low temperatures, the proposed room-temperature bonding strategy guarantees the mechanical property of the material, as well as high-resolution channel geometries. Also, due to the high robustness of the bonding achieved, the proposed bonding strategy is particularly suited for microfluidic experiments where high internal fluid pressure is required, such as in liquid chromatographic applications and microreactors. When combined with a flexible PDMS

substrate, the hybrid plastic–PDMS system introduced in this study could provide a useful platform for cell-based research owing to the less hydrophobic property of plastic materials as well as their versatility, combined with fluid actuation components such as microvalves and micropumps provided by the elastomeric nature of PDMS. This could pave the way for a simplified construction of a disposable microfluidic platform, where selectively patterned or pre-dispensed cells, biomolecules, and biochemical reagents, as well as an encapsulation of micro- or nanoparticles, are required prior to sealing. Also, room temperature packaging of integrated circuit (IC)-patterned polyimide substrates will be possible for realizing flexible display technologies.

## Acknowledgements

## Notes and references

1 L. Martynova, L. E. Locascio, M. Gaitan, G. W. Kramer, R. G. Christensen and W. A. MacCrehan, *Anal. Chem.*, 1997, **69**, 4783–4789.
2 L. J. Kricka, P. Fortina, N. J. Panaro, P. Wilding, G. Alonso-Amigo and H. Becker, *Lab Chip*, 2002, **2**, 1–4.
3 G.-B. Lee, S.-H. Chen, G.-R. Huang, W.-C. Sung and Y.-H. Lin, *Sens. Actuators, B*, 2001, **75**, 142–148.
4 R. M. McCormick, R. J. Nelson, M. G. Alonso-Amigo, D. J. Benvegnu and H. H. Hooper, *Anal. Chem.*, 1997, **69**, 2626–2630.
5 A. Wainright, U. T. Nguyen, T. Bjornson and T. D. Boone, *Electrophoresis*, 2003, **24**, 3784–3792.
6 Y. Sun, Y. C. Kwok and N.-T. Nguyen, *J. Micromech. Microeng.*, 2006, **16**, 1681–1688.
7 R. T. Kelly and A. T. Woolley, *Anal. Chem.*, 2003, **75**, 1941–1945.
8 J. Chen, M. Wabuyele, H. Chen, D. Patterson, M. Hupert, H. Shadpour, D. Nikitopoulos and S. A. Soper, *Anal. Chem.*, 2005, **77**, 658–666.
9 L. Brown, T. Koerner, J. Hugh Horton and R. D. Oleschuk, *Lab Chip*, 2006, **6**, 66–73.
10 C. Lucio do Lago, H. D. Torres da Silva, C. A. Neves, J. G. Alves Brito-Neto and J. A. Fracassi da Silva, *Anal. Chem.*, 2003, **75**, 3853–3858.
11 B. H. Weigl, R. Bardell, T. Schulte, F. Battrell and J. Hayenga, *Biomed. Microdevices*, 2001, **3**, 267–274.
12 L. Song, D. Fang, R. K. Kobos, S. J. Pace and B. Chu, *Electrophoresis*, 1999, **20**, 2847–2855.
13 J. Xu, L. Locascio, M. Gaitan and C. S. Lee, *Anal. Chem.*, 2000, **72**, 1930–1933.
14 W. W. Y. Chow, K. F. Lei, G. Shi, W. J. Li and Q. Huang, *Smart Mater. Struct.*, 2006, **15**, S112–S116.
15 H. Wu, B. Huang and R. N. Zare, *Lab Chip*, 2005, **5**, 1393–1398.
16 J. W. Suk, J.-Y. Jang and J.-H. Cho, *J. Micromech. Microeng.*, 2008, **18**, 055024.
17 M.-E. Vlachopoulou, A. Tserepi, P. Pavli, P. Argitis, M. Sanopoulou and K. Misiakos, *J. Micromech. Microeng.*, 2009, **19**, 015007.
18 D. C. Duffy, J. C. McDonald, O. J. A. Schueller and G. M. Whitesides, *Anal. Chem.*, 1998, **70**, 4974–4984.
19 N. Y. Lee and B. H. Chung, *Langmuir*, 2009, **25**, 3861–3866.
20 N. Y. Lee and Y. S. Kim, *Macromol. Rapid Commun.*, 2007, **28**, 1995–2000.
21 J. Park, Y. S. Kim and P. T. Hammond, *Nano Lett.*, 2005, **5**, 1347–1350.
22 D. Raghavan, M. VanLandingham, X. Gu and T. Nguyen, *Langmuir*, 2000, **16**, 9448–9459.
23 L. Brown, T. Koerner, J. Hugh Horton and R. D. Oleschuk, *Lab Chip*, 2006, **6**, 66–73.
24 Z. Wang and R.-X. Li, *Nanoscale Res. Lett.*, 2007, **2**, 69–74.
25 L. Y. L. Wu, L. Boon, Z. Chen and X. T. Zeng, *Thin Solid Films*, 2009, **517**, 4850–4856.
26 J. Chai, F. Lu, B. Li and D. Y. Kwok, *Langmuir*, 2004, **20**, 10919–10927.
27 Q. Wei, Y. Liu, D. Hou and F. Huang, *J. Mater. Process. Technol.*, 2007, **194**, 89–92.
28 B. Zhu, H. Iwata, I. Hirata and Y. Ikada, *J. Adhes. Sci. Technol.*, 2000, **14**, 351–361.
29 Y.-S. Lin and H.-M. Liu, *Thin Solid Films*, 2008, **516**, 1773–1780.
30 V. V. Tsukruk and V. N. Bliznyuk, *Langmuir*, 1998, **14**, 446–455.
31 A. Heise, H. Menzel, H. Yim, M. D. Foster, R. H. Wieringa, A. J. Schouten, V. Erb and M. Stamm, *Langmuir*, 1997, **13**, 723–728.
32 D. F. Siqueira Petri, G. Wenz, P. Schunk and T. Schimmel, *Langmuir*, 1999, **15**, 4520–4523.
33 M. A. Eddings, M. A. Johnson and B. K. Gale, *J. Micromech. Microeng.*, 2008, **18**, 067001.
34 N. Y. Lee, J. R. Lim, M. J. Lee, S. Park and Y. S. Kim, *Langmuir*, 2006, **22**, 7689–7694.
35 S. F. Li and S. C. Chen, *IEEE Trans. Adv. Packag.*, 2003, **26**, 242–247.
36 S. K. Sia and G. M. Whitesides, *Electrophoresis*, 2003, **24**, 3563–3567.